Chapter 30
On Brake Pad Shim Characterization: a Homogenization Approach and Finite Element Analysis

Dominik Schmid, Nils Gräbner & Utz von Wagner

Abstract Brake squeal is a typical problem of "Noise, Vibration, Harshness" (NVH) phenomena in the automotive world leading to potential customer complaints. This high frequency noise in the audible frequency range of approximately 1 kHz to 15 kHz is induced by self excitation resulting from the frictional contact between brake pad and disk. A typical industrial countermeasure to address this problem is the mounting of thin composite structures consisting of elastomer and steel layers, so called shims, on the pad backplates. They are applied to increase the damping and to influence the vibration shapes.
The computational modeling of shims using Finite Elements is still a complex task and shows significant potential for improvement. To avoid problems resulting from element sizes of the partially very thin layers a classical homogenization theory from literature is considered. This homogenization approach maps shim properties in an improved manner which contributes to substantially smaller model sizes as well as less simulation effort and time. Therefore, analytical approaches for constrained layer damping structures are introduced and corresponding theoretical results are presented. To validate these theoretical results, experimental investigations are carried out on shims bonded to structures, especially steel plates and brake pads.

Keywords: Shims · Constrained layer damping · Homogenization · Finite Element simulation · NVH

Dominik Schmid · Nils Gräbner · Utz von Wagner
Chair of Mechatronics and Machine Dynamics, Technische Universität Berlin, 10587 Berlin, Germany,
e-mail: dominik.schmid@tu-berlin.de, nils.graebner@tu-berlin.de, utz.vonwagner@tu-berlin.de

B. E. Abali et al. (eds.), *New Achievements in Continuum Mechanics and Thermodynamics*, Advanced Structured Materials 108,
https://doi.org/10.1007/978-3-030-13307-8_30

30.1 Introduction

Numerous technical applications especially in lightweight structures nowadays require high stiffness characteristics with simultaneously high damping ratios in order to avoid undesired vibrations. A typical example for fulfilling such requirements is the application of composites. These structures meet the requirements by exhibiting good damping behavior without loosing stiffness (Marcelin et al, 1995). The application of such composites called shims on brake pad backplates is a typical countermeasure against undesired vibration phenomena like brake squeal. Brake squeal is a high frequency noise in the audible frequency range of approximately 1 kHz to 15 kHz based on self-excited vibrations caused by friction forces between pad and disk (Kinkaid et al, 2003; Cantoni et al, 2009). Shims are thin layer bonded structures consisting of viscoelastic elastomer layers and steel plates with high stiffness. Figure 30.1 shows the general set-up of a brake pad with shim consisting of the friction material being in contact with the disk during the braking process, the backplate and the shim, which is coupled to the backplate by an adhesive layer. Designing and selecting appropriate shims is still a major task to solve. There are plenty of experimental investigations required to find the right shim matching the individual noise problems of the respective brake. This includes the experimental investigation of the components as well as dynamometer tests of the entire brake and tests in the vehicle.

A standard industrial tool in the investigation of brake squeal is the so-called complex eigenvalue analysis (CEA). The CEA is based on large Finite Element models of the entire brake with disk, pads, caliper, carrier and the suspension. Equilibrium positions resulting from the applied brake torque are calculated by a static analysis and the equations of motion are linearized with respect to them (Gräbner et al, 2016). Gyroscopic terms and, due to the friction forces between disk and pads circulatoric terms, i.e. self excitation, is present. This may result in positive real parts of the eigenvalues, i.e. instability of the aforementioned equilibrium solution. Therefore the overall goal of CEA is to characterize the stability behavior of equilibrium solutions of brake systems as an indicator for possible onset of squeal. The accurate calculation of the eigenvalues anyway is a challenging problem (Gräbner et al, 2016) for that large gyroscopic-circulatory systems. The squealing itself is a limit cycle oscillation requiring to consider nonlinearities (Gräbner et al, 2014) and corresponding bifurcation behavior.

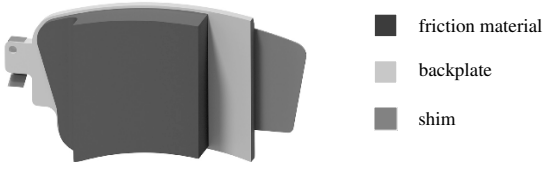

Fig. 30.1 Brake pad composition (Schmid, 2018a)

Damping is well known to influence and to be able to suppress self-excited vibrations, see e.g. (Gräbner et al, 2015) both in the linear as well as in the nonlinear case. On the other hand, damping is hard to identify and therefore in many applications only estimated or even neglected. Neglected or underestimated damping in general leads to overestimated eigenvalues with positive real parts and corresponding potential squeal frequencies. Therefore, modeling of damping, at least for components introduced by intention in order to damp vibrations like the shims, is a key issue for improved modeling of the system's behavior. Hereby, mapping the damping capacity of the shim's viscoelastic layer is an essential point. Compared to the overall high amount of literature on brake squeal including several review papers like the already mentioned in Kinkaid et al (2003) and Cantoni et al (2009) publications on modeling of shims are somewhat rare. Examples for FE investigations including shims are in Festjens et al (2012) and Kang (2012). Esgandari and Olatunbosun (2016) implemented Rayleigh damping in elastomer layers of shims, steel layers are still undamped. Rayleigh parameter are used based on previous investigations from Flint et al (2004). There are also some technical standards on shims like in SAE-J3001 (2011).

The problem in including the shims in FE-models are the thin layers in shims, which in general may have thicknesses in the range of 0.1 mm. Using element sizes in the same range with, in the FE sense "healthy", ratios of element dimensions would lead to element numbers which cannot be handled, if complete models of the entire brake are considered.

Therefore, the basic idea of the work described in this paper is, to homogenize the shim layered structure using classical theories and approaches. This is done in order to enable larger element sizes allowing for acceptable numbers of degrees of freedom, which can be handled in models of the entire brake. In this contribution shims with two thin elastomer layers enclosed by a metal core are examined in detail.

There is a large number of publications on the dynamics of composites combining metal and elastomer layers. One of the first theories has been published in the middle of the last century by Oberst describing unconstrained damping treatments (Oberst and Frankenfeld, 1952; Oberst et al, 1954). The purpose was to homogenize structures consisting of layers with different characteristics. As a result a single layer with equivalent mechanical properties describing stiffness and damping ratios is obtained. Characterizing system properties analytically Kerwin extended Oberst's theory considering an additional stiff top layer Kerwin Jr (1959) which in the following was called constrained layer. The energy dissipation for constrained layer compounds is mainly induced by shearing of the viscoelastic core material and exceeds the extensional damping of unconstrained damping treatments Ross et al (1959). The developed theory for free vibrations was introduced for fully coverage of the damping and constraining layer considering pinned-pinned boundary conditions. DiTaranto also addressed this problem and developed a sixth order equation for longitudinal displacement. He formulates the loss factor for coverage of the entire beam for any boundary condition (DiTaranto, 1965). The transverse displacement of beams with damping treatments has been published by Mead and Markuš

for arbitrary boundary conditions and has been extended for forced vibrations (Mead and Markuš, 1969) and (Mead and Markuš, 1970). Using an energy approach an exact solution for the sixth order equation as well as numerical approaches were described by Rao (Rao, 1978).

The publications listed so far require full coverage of all layers. In general brake pads used in vehicles show only partial coverage of shims bonded to back plates. The more general set-up of only partial coverage has been investigated by Nokes describing damping of beams for any symmetrical boundary conditions requiring a centered constrained layer on the structure (Nokes and Nelson, 1968). Markuš (1974) dealed with the damping mechanism of beams and developed a theory for partially covered constrained layers predicting damping for any boundary conditions. Damping material calculation formulas of sandwich beams with partially covering damping layers have been presented by Sylwan achieving equal damping properties compared to full coverage (Sylwan, 1978). Moreover two approximate solutions and one exact method for the damping description of partially covered sandwich beams have been published by Lall et al (1988). Flint presents essential publications in his PhD thesis considering full coverage (Flint, 2002). An overview and classification of relevant surface damping treatments can be found in the books from Nashif et al (1985) and Sun and Lu (1995).

The aim of this contribution is to carry out Finite Element simulations of homogenized shims with a view to less experimental effort and better prediction quality. With this stiffness characteristics of shims and in particular loss factors of shims bonded to rectangular steel plates are determined analytically and applied to an Abaqus CAE model. The loss factors for full coverage are compared considering torsional and flexural mode shapes. The damping behavior of the viscoelastic core is implemented in a Finite Element model. As a further step towards the improved shim modeling, brake pads are examined numerically. Furthermore, concrete recommendations on modeling and meshing shims are introduced. Finally experimental investigations are carried out to validate damping and stiffness characteristics using methods as described in SAE guideline J3001 (SAE-J3001, 2011).

30.2 Modeling of Shims

The dynamical characterization of shims includes modal parameters like natural frequencies, mode shapes and damping ratios. The focus is to map torsional and bending modes analytically. Therefore, mechanical models focusing on stiffness and damping behavior of shims are examined. Following most set-ups in literature and in order to prevent influence resulting from the support, which may affect natural frequencies and damping characteristics, a free-free support is utilized for modeling and experimental investigations (Ewins, 1984) in the following. These boundary conditions will of course change, if the resulting pad and shim model will be integrated into the model of the entire brake.

30.2.1 Continuous Mechanical Systems

For introduction classical models for torsional vibrations of bars as well as Euler-Bernoulli beams with a rectangular cross section are reconsidered in the following, where the corresponding formulas can be taken from textbooks, e.g. Hagedorn and DasGupta (2007). A free-free torsional bar is shown in Fig. 30.2, where G is the shear modulus, ϱ the mass density as well as I_P and I_T are the polar and torsional moments of inertia respectively. Describing the geometrical dimensions of the bar, the length l, the width b and height h are introduced. The following partial differential equation describes the torsional free vibrations $\vartheta(x,t)$ of the bar with uniform cross section by

$$\frac{\partial^2 \vartheta}{\partial t^2} - c^2 \frac{\partial^2 \vartheta}{\partial x^2} = 0, \tag{30.1}$$

where c is the wave propagation speed for the torsional vibrations with

$$c^2 = \frac{G\, I_\mathrm{T}}{\varrho\, I_\mathrm{P}}. \tag{30.2}$$

Taking the boundary conditions of the system $\vartheta'(0,t) = 0$ and $\vartheta'(l,t) = 0$ into account, the natural frequencies f_{tn} can be determined as

$$f_{tn} = \frac{n\, c}{2\, l} \quad \forall\, n \in \mathbb{N}. \tag{30.3}$$

In general for isotropic materials, G can be expressed by the respective Young's modulus E and the Poisson's ratio ν

$$G = \frac{E}{2\,(1+\nu)}. \tag{30.4}$$

A rectangular Euler-Bernoulli beam executing lateral vibrations is sketched in Fig. 30.3. The corresponding partial differential equation describing lateral free vibrations $w(x,t)$ of an Euler-Bernoulli beam with uniform cross section is given by

$$\frac{\partial^2 w}{\partial t^2} + \frac{E I_\mathrm{y}}{\varrho\, A} \frac{\partial^4 w}{\partial x^4} = 0. \tag{30.5}$$

The equation includes the flexural rigidity with the geometrical moment of inertia I_y and the area A. With the free-free boundary conditions $w''(0,t) = 0$, $w''(l,t) = 0$, $w'''(0,t) = 0$ and $w'''(l,t) = 0$ the natural frequencies can be determined in the

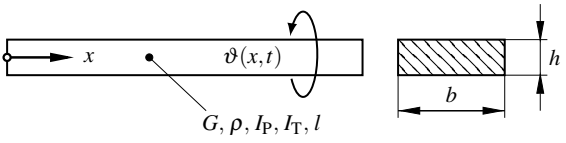

Fig. 30.2 Rectangular free-free bar

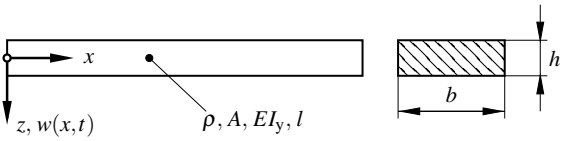

Fig. 30.3 Free-free Euler-Bernoulli beam

following form considering correction terms e_n Hagedorn and DasGupta (2007)

$$f_{\mathrm{b}n} = \frac{1}{2\,\pi}\left(\frac{2\,n+1}{2}\,\pi + e_n\right)^2 \frac{1}{l^2}\sqrt{\frac{E\,I_{\mathrm{y}}}{\varrho\,A}} \quad \forall\, n \in \mathbb{N} \tag{30.6}$$

with $e_1 = 0.01766$ and $e_2 = -0.00078$. Results determined using this approach are denoted as "analytical homogenized" (analytical hom) in Sect. 30.5.

30.2.2 Constrained Layer Damping Theory

In contrast to free layer damping, where the extension of the composite caused by length change due to bending is responsible for the damping behavior, constrained layer damping treatments, in the following denoted as CLD approach, are more complicated to describe. Shearing of the viscoelastic layer, which is the main mechanism of energy dissipation, is induced due to the deflection of both elastic layers. The investigated assembly is illustrated in Fig. 30.4. The following theory is based on the formulations of Rao Rao (1978). The damping mechanism of the elastomer layer is characterized by the complex dynamic shear modulus in Eq. (30.7), where η_2 is the core loss factor and G_2 the elastic shear modulus Leaderman (1949). Here and in the following all parameters marked with * denote complex numbers:

$$G_2^* = G_2(1 + \mathrm{i}\,\eta_2). \tag{30.7}$$

Classifying and comparing the computed results with data from literature, loss factors of metals lie between 10^{-4} and 10^{-3} approximately, whereas polymers can be expected to possess loss factors in the range of 10^{-1} to $2 \cdot 10^0$, see Oberst (1956)

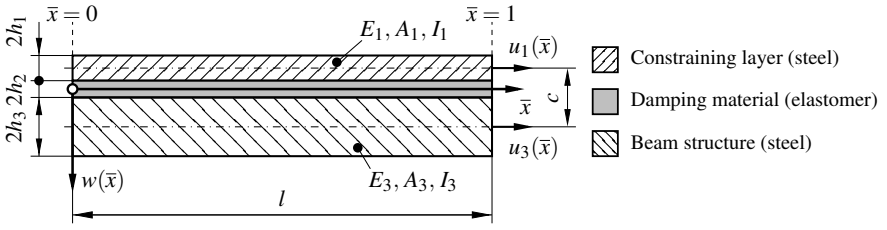

Fig. 30.4 Constrained layer damping with full coverage, according to Rao (1978)

and Beranek and Vér (1992); in some sources polymer loss factors are specified even up to 10^1 Ottl (1981). For describing flexural modes the main assumptions for the isotropic and homogeneous layers are according to Rao (1978):

- small beam deflections are considered which are determined using Euler-Bernoulli hypothesis
- the elastomer core layer is sheared which is the main energy dissipation mechanism
- longitudinal displacements of layers are continuous
- longitudinal and rotatory inertia effects are neglected

Ross, Kerwin and Ungar as well as other authors like Nokes and Nelson assumed, that mode shapes of the beam are unaffected by the damping treatment Kerwin Jr (1959) and Nokes and Nelson (1968). This fact was also confirmed experimentally in this contribution. Constrained layer damping theories consider the longitudinal displacements of the elastic layers u_1 and u_3 as well as the vertical displacement of the beam structure w. Characteristic sandwich equations can be formulated in terms of the transverse deflection $w(\overline{x}, \overline{t})$ only

$$-\frac{\partial^6 w}{\partial \overline{x}^6} + g^*(1+Y)\frac{\partial^4 w}{\partial \overline{x}^4} - \frac{\partial^4 w}{\partial \overline{t}^2 \partial \overline{x}^2} + g^*\frac{\partial^2 w}{\partial \overline{t}^2} = 0. \tag{30.8}$$

where $\overline{x}$ and $\overline{t}$ constitute normalized space and time coordinates as well as Y and g^* constitute geometric and shear parameters as

$$Y = \frac{(h_1 + h_3 + 2\,h_2)^2}{E_1\,I_1 + E_3\,I_3}\,\frac{E_1\,A_1\,E_3\,A_3}{E_1\,A_1 + E_3\,A_3}, \tag{30.9}$$

$$g^* = \frac{G_2^*\,A_2\,l^2}{4\,h_2^2}\,\frac{E_1\,A_1 + E_3\,A_3}{E_1\,A_1\,E_3\,A_3}. \tag{30.10}$$

Solving the sixth order partial differential equation the ansatz (30.11) can be used. A complex exponential ansatz for $w_m(\overline{x}, \overline{t})$ is assumed, where k_n^* are characteristic values, A_m the coefficients and Ω_m^* the complex frequency factors

$$w_m(\overline{x}, \overline{t}) = \sum_{n=1}^{6} A_m\,\mathrm{e}^{k_n^* \overline{x}}\,\mathrm{e}^{\Omega_m^* \overline{t}}. \tag{30.11}$$

Substituting (30.11) in (30.8) yields the characteristic equation

$$-k_n^{*\,6} + g^*(1+Y)k_n^{*\,4} + \Omega_m^{*\,2}(k_n^{*\,2} - g^*) = 0. \tag{30.12}$$

Solving the polynomial (30.12) for k_n^*, three square-roots are obtained depending on the frequency factor Ω_m^*. This parameter includes the angular frequency Ω_m of the sandwich compound and the loss factor $\eta_{\text{struc},m}$ of the entire structure.

$$\Omega_m^* = \Omega_m\sqrt{1 + \mathrm{i}\,\eta_{\text{struc},\,m}} \tag{30.13}$$

The sixth order differential Eq. (30.8) for full coverage requires six boundary conditions, three for each end of the beam to determine the unknown coefficients A_1 to A_6. For a structure with unrestrained free ends there is no bending moment and shear force at the left end ($\overline{x} = 0$) and right end ($\overline{x} = 1$) of the beam. Additionally, the normal force is zero. The free-free unrestrained boundary conditions are given by

$$w_m^{\mathrm{IV}}(\overline{x}) - g^*(1+Y)w_m^{\mathrm{II}}(\overline{x}) - \Omega_m^{*2}\, w_m(\overline{x}) = 0, \tag{30.14}$$

$$w_m^{\mathrm{V}}(\overline{x}) - g^*(1+Y)w_m^{\mathrm{III}}(\overline{x}) - \Omega_m^{*2}\, w_m^{\mathrm{I}}(\overline{x}) = 0, \tag{30.15}$$

$$w_m^{\mathrm{IV}}(\overline{x}) - g^*\, Y\, w_m^{\mathrm{II}} - \Omega_m^{*2}\, w_m(\overline{x}) = 0. \tag{30.16}$$

These six equations can be transferred in a linear, homogeneous system of equations, where $\mathbf{M}_{\mathrm{A}}$ defines a square matrix and $\mathbf{a}$ is the vector of unknown coefficients A_1 to A_6

$$\mathbf{M}_{\mathrm{A}}\, \mathbf{a} = \mathbf{0}. \tag{30.17}$$

To obtain non-trivial solutions $\mathbf{a}$ the determinant of $\mathbf{M}_{\mathrm{A}}$ has to be zero. Analytical determined frequencies and loss factors are compared with experimental investigations to verify the prediction quality of this approach.

30.3 Experimental Investigations

Measuring modal parameters the test rig in Fig. 30.5 is used, considering standard methods as e.g. described in the SAE test procedure J3001 SAE-J3001 (2011). To prevent double hits during excitation, an automatic impulse hammer 1) is applied. The system response has been measured in point 2) by using a single point laser vibrometer detecting the velocity of the measurement objects in out of plane direction. To minimize the influence of the support, the test object is suspended (hung up) in a frame by strings. The investigations included shims bonded to rectangular steel

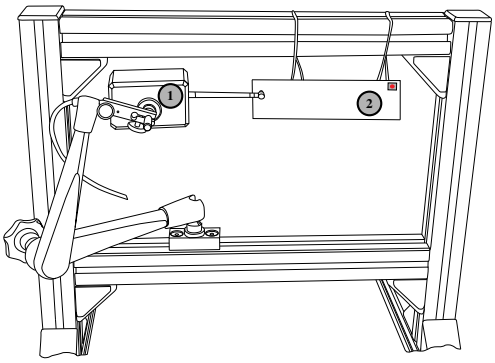

Fig. 30.5 Experimental set-up for shim investigations Schmid (2018b)

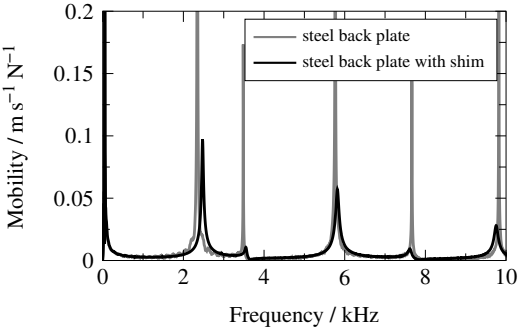

Fig. 30.6 Mobility of shims bonded to structure

plates with dimensions $180\text{x}50\text{x}5\,\text{mm}^3$ as well as brake pads with identical shims. Examining full coverage of the base structure shims are applied having equal length and width dimensions. A transfer function for one shim type bonded to brake pad backplates is illustrated in Fig. 30.6 in the range up to 10 kHz. These transfer functions are the basis for determining modal damping values for flexural and torsional mode shapes. The half-power bandwidth method has been applied for all damping ratios ϑ, considering a 3 dB decay logarithmically seen in equation

$$2\,\vartheta = \frac{1}{2}\left[\left(\frac{\Omega_\mathrm{o}}{\omega_\mathrm{d}} - \frac{\omega_\mathrm{d}}{\Omega_\mathrm{o}}\right) - \left(\frac{\Omega_\mathrm{u}}{\omega_\mathrm{d}} - \frac{\omega_\mathrm{d}}{\Omega_\mathrm{u}}\right)\right] \tag{30.18}$$

for nonsymmetrical transfer functions where ϑ is the modal damping ratio, ω_d the natural angular frequency and $\Omega_{\mathrm{o,\,u}}$ are angular frequencies determined from the transfer functions Beards (1983). The first four eigenmodes of a rectangular plate are presented in Fig. 30.7. Torsional and flexural mode shapes alternate for the first eight eigenfrequencies. Odd numbered natural frequencies represent bending modes, whereas even numbered modes correspond to torsion. Additional parameters playing an important role to obtain a more realistic mapping are the stress history and temperature impact on elastomers (Lazan, 1968), which we intend to address in future investigations. Also the rheological behavior of the viscoelastic layer may play an important role (Jones, 2001).

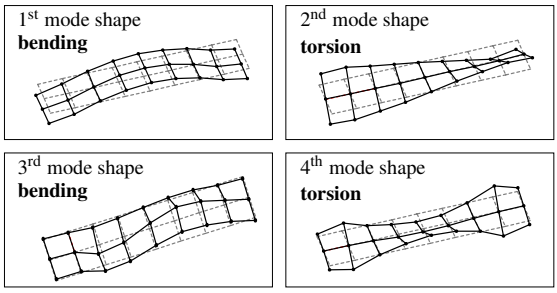

Fig. 30.7 Experimentally identified mode shapes of shims bonded to steel plates

30.4 Finite Element Approach

In the following multi- and single-layer shim structures are analyzed based on theories from literature applied to our shim problem. Corresponding FE results are denoted in Sect. 30.5 as "FE multilayer" and "FE hom" depending on the number of layers. The aim hereby is to map shims as homogenized entity to avoid modeling problems resulting from the layer thickness. As a simulation tool for modeling the shims and carrier structures, Abaqus CAE is used. All results have been produced using frequency and complex frequency steps of the implicit solver Abaqus/Standard. Specifically the Lanczos solver is used for this task Lanczos (1950).

30.4.1 Damping

Several aspects and problems of modeling damping in FE-models of brakes have been addressed in Gräbner et al (2015). Structural (30.19) as well as Rayleigh damping (30.20) are integrated for shim structures in Abaqus

$$\mathbf{M}\,\ddot{\mathbf{q}} + \mathbf{K}(1 + \mathrm{i}\beta_{\text{struc.}})\mathbf{q} = \mathbf{f}, \tag{30.19}$$

$$\mathbf{M}\,\ddot{\mathbf{q}} + (\alpha\,\mathbf{M} + \beta\,\mathbf{K})\dot{\mathbf{q}} + \mathbf{K}\,\mathbf{q} = \mathbf{f}. \tag{30.20}$$

These are linear systems of differential equations, where $\mathbf{q}$ is the displacement vector as a function of time, $\mathbf{M}$ the mass matrix, $\mathbf{K}$ the stiffness matrix and $\mathbf{f}$ the excitation vector. Instead of using a classical damping matrix for the energy dissipation, a complex stiffness matrix for structural damping is considered with the damping parameter $\beta_{\text{struc.}}$ of the material. For Rayleigh damping α and β are introduced to influence the damping behavior. This damping type is a mathematical construct weighting the impact of mass and stiffness matrices. The influence of α and β on the damping ratio ϑ can be calculated from Eq. (30.21) (Zienkiewicz, 1977), where ω_0 is the natural angular frequency of the system

$$\vartheta = \frac{\alpha + \beta\,\omega_0^2}{2\,\omega_0}. \tag{30.21}$$

Rayleigh damping is implemented for homogenized structures and the friction material separately, whereas layer bonding structures are described using structural damping for metal layers and viscoelastic layers. Figure 30.8 outlines a Rayleigh fit for experimental results which are shown as round marks. Therefore, a least squares fitting method (FindFit), which is implemented in Wolfram Mathematica is used. Using experimental modal analysis, statistical evaluations have shown, that samples of formal identical brake pads have a slight variance in natural frequencies and a serious variance in damping ratios. Deviations of almost 20% are identified regardless

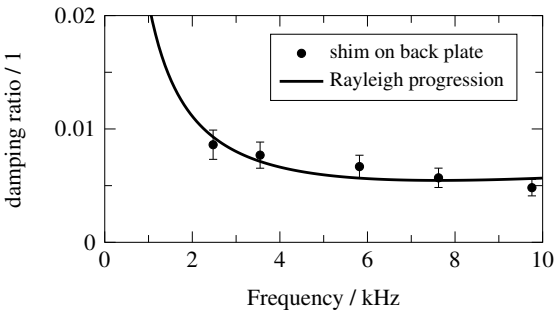

Fig. 30.8 Approximation of experimental modal damping ratios

of the mode shape. Hence, the implementation of the exact dissipation parameter is not expedient and justifies the Rayleigh approach.

30.4.2 Stiffness - Homogenization Theory

In the following the theory from Ross et al (1959) is used for the improved modeling of shims. The technique is based on summarizing elastic and viscoelastic layers up to one single layer with equivalent properties. This homogenization requires homogeneous single layers for creating a body with equal mechanical properties including density, thickness, stiffness and damping features, as shown in Fig. 30.9 schematically. Stiffness characteristics mainly come from the metal layers, in particular the base beam, whereas the structure loss factor depends on the shearing of the elastomer coating. This theory requires geometrical information about each layer as well as rheological specifications like material properties. Isotropic material behavior is required to all further computations. Therefore, the overall density and the replacement of Young's modulus of the compound is implemented for improved computations. Poisson ratio effects coming from the homogenization are neglectable for FE-simulations. The Poisson's ratio ν of the homogenization structure is assumed to be 0.3 corresponding to the elastic layers. In general the Poisson's ratio of elastomers is specified by 0.5 in literature. Avoiding numerical issues in FE calculations the Poisson's ratio of each viscoelastic layer is defined here as 0.49.

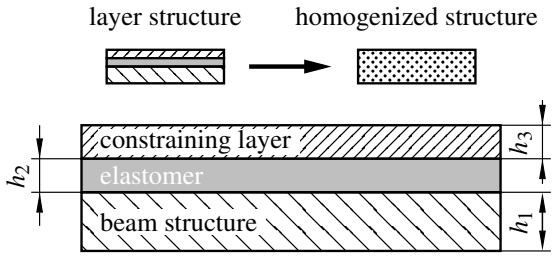

Fig. 30.9 Homogenization of a three layer compound

Shims, examined in more detail, consist of a stiff steel structure (constraining layer) and elastomer layers. Note that the homogenization includes the beam structure, the elastomer layer and the constraining layer. Adhesive layers and further top layers have to be modeled additionally. Equation (30.22) shows the flexural rigidity ratio $E\,I$ of the homogenized structure

$$\begin{aligned} E\,I = {} & E_1 \frac{h_1^3}{12} + E_2 \frac{h_2^3}{12} + E_3 \frac{h_3^3}{12} - E_2 \frac{h_2^2}{12} \left(\frac{h_{31} - D}{1+g} \right) + E_1\, h_1\, D^2 \\ & + E_2\, h_2\, (h_{21} - D)^2 + E_3\, h_3\, (h_{31} - D)^2 \\ & - \left(\frac{E_2\, h_2}{2} (h_{21} - D) + E_3\, h_3 (h_{31} - D) \right) \left(\frac{h_{31} - D}{1+g} \right). \end{aligned} \tag{30.22}$$

The resulting composite with only one layer considers the thickness diversity of the steel and viscoelastic layer, where E is the Young's modulus, h the thickness of each layer shown in Fig. 30.9, I the corresponding geometrical moment of inertia, p the wave number (eigenvalue per length) and G_2 the shear modulus of the viscoelastic core as seen in Eq. (30.23) Nashif et al (1985).

$$D = \frac{E_2\, h_2 \left(h_{21} - \frac{h_{31}}{2} \right) + g(E_2\, h_2\, h_{21} + E_3\, h_3\, h_{31})}{E_1\, h_1 + \frac{1}{2} E_2\, h_2 + g(E_1\, h_1 + E_2\, h_2 + E_3\, h_3)} \tag{30.23}$$

with the parameters:

$$h_{31} = \frac{1}{2}(h_1 + h_3) + h_2 \tag{30.24}$$

$$h_{21} = \frac{1}{2}(h_1 + h_2) \tag{30.25}$$

$$g = \frac{G_2}{E_3\, h_3\, h_2\, p^2}. \tag{30.26}$$

If there is no width difference between the single layers, the resulting Young's modulus only depends on thickness and elasticity ratios. The homogenization properties received are used for analytical and numerical models.

30.4.3 Modeling

Common problematic issues in modeling shims on brake pads, e. g. hourglass effects, may result from the selection of inappropriate element types as shown in Fig. 30.10. Often, reduced elements or elements without using hourglass control lead to zero energy modes which can be checked easily by inspecting the mode shapes. Moreover, the meshing of composite shim structures has to be done with high accuracy due to the layer thickness. A massive increase in degrees of freedom entails inevitably. The investigated shim type consists of one steel and two elastomer

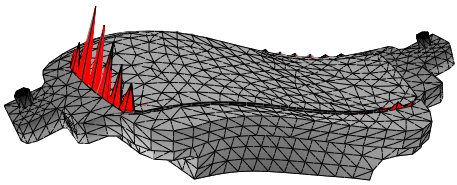

Fig. 30.10 Hourglass effect occuring at FE model with non-homogenized shim

layers one on each side, which is bonded on rectangular steel plates and backplates of brake pads. Figure 30.11 shows two test objects, the multilayer mesh compound and the homogenized structure. For layer bonding structures the components are as-

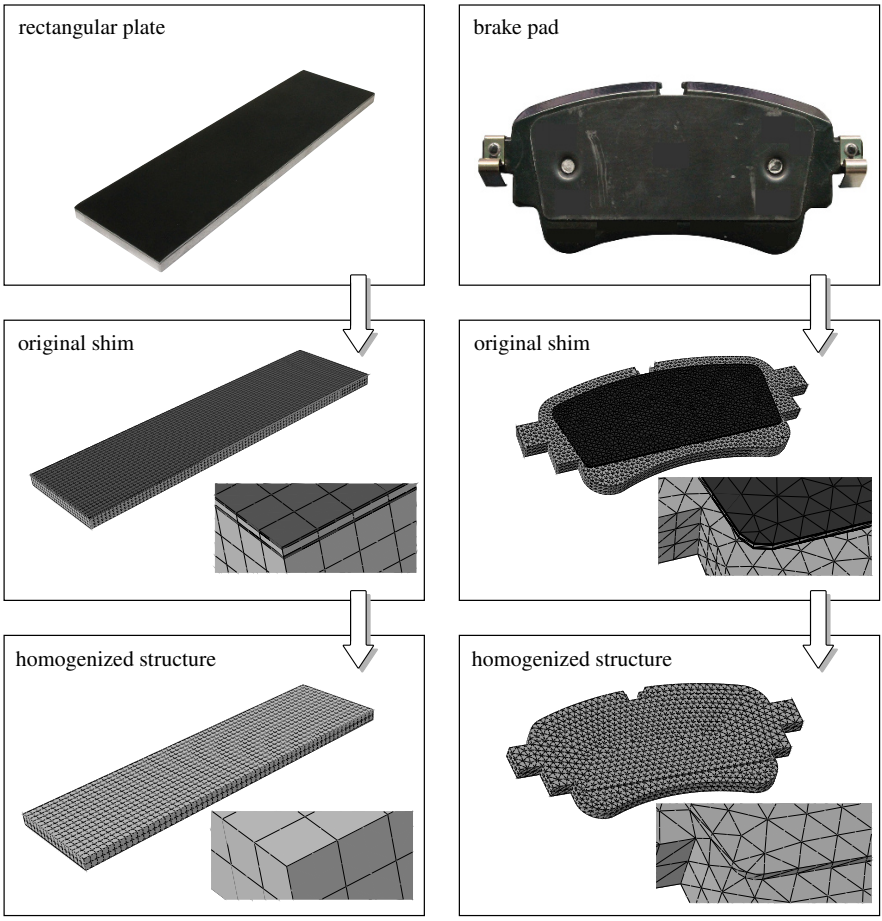

Fig. 30.11 FE modeling before and after having applied the homogenization theory to rectangular plates and brake pads

sembled using tie constraints. Solid as well as shell elements with eight nodes (S8R) are used for modeling steel plates and modified shim parts. Brake pad backplates are meshed exclusively with solid elements. When implementing the improved brake pad in a FE brake model, solid elements are recommended to be used due to several interactions of the brake pad in further steps. An examination on hexahedron elements with linear (C3D8) and quadratical (C3D20) approach has been carried out. To analyze the mesh influence a convergence analysis has been carried out with the original shim structure and after having applied the homogenization theory from Ross-Kerwin-Ungar. Thus, the element length is varied that leads to an aspect ratio of approximately 1:40 to 1:1 considering the thickness of the unmodified shim compound. The same element length has been applied for each layer. Quadratical elements show a very good convergence for computed natural frequencies even for a coarse mesh. Whereas the elements with linear approach need to be meshed with much smaller element length achieving the same results. This is due to the fact that additional middle nodes for each element map the shearing of structures more detailed. Note that higher mode shapes need to be computed with smaller aspect ratios to achieve a convergence behavior. Consequently for thin structures the quadratical approach is recommended to use.

30.5 Results and Validation

Results of the described methods for the investigated shim type in the range up to $5\,\mathrm{kHz}$ for a fully covered rectangular steel plate and in the range up to $10\,\mathrm{kHz}$ for a brake pad are shown in Table 30.1. An analytical constrained layer damping approach (CLD approach) for bending shapes, classical analytical calculations for homogenized structures (Sect. 30.2.1), Finite Element computations comparing the homogenized and the layered shim structure are demonstrated. In Abaqus implementing Rayleigh as well as structural damping in the investigated structures has been focused. The extension on brake pads has been carried out considering a higher degree of complexity including geometry and the influence of the lining.

To validate the approaches, results from experimental modal analyses are shown. Thus, loss factors of elastomers often depend on frequency (temperature) and amplitude Crandall (1970), all experimental investigations are carried out at room temperature (23^0). Natural frequencies and characteristic loss factors are listed in Table 30.1. The experimental loss factors are determined having regard to the power-bandwidth method from Eq. (30.18).

Overall, natural frequencies of Finite Element computations yield a very good compliance with experimental investigations. In particular loss factors of the rectangular beam and shim modeled as several monolayers overestimate the damping behavior from the second mode shape. Structural damping only showed good results for the backplate. In both homogenized single layer test structures the implemented Rayleigh-damping showed a very good agreement with experimental determined loss factors. Solid as well as shell elements deliver excellent results and map the

Table 30.1 Comparison of shim natural frequencies and loss factors for a free-free support

Object	Method	f_1 [a] / Hz	η_1 -	f_2 [b] / Hz	η_2 -	f_3 [a] / Hz	η_3 -	f_4 [b] / Hz	η_4 -	f_5 [a] / Hz	η_5 -
steel plate	Experimental	819	0.008	1769	0.004	2244	0.004	3663	0.003	4381	0.001
steel plate	Experimental	872	0.014	1809	0.018	2341	0.019	3722	0.016	4472	0.022
with shim	FE multi layer*	878	0.014	1780	0.025	2353	0.025	3672	0.025	4494	0.027
	FE hom*	847	0.017	1788	0.014	2333	0.015	3714	0.019	4551	0.023
	FE hom**	847	0.017	1787	0.014	2332	0.015	3711	0.019	4548	0.022
	CLD approach	881	0.009	-	-	2367	0.019	-	-	4525	0.021
	Analytical hom	848	-	1763	-	2347	-	3526	-	4595	-
backplate	Experimental	2348	0.003	3483	0.002	5766	0.001	7664	0.001	9820	0.001
backplate	Experimental	2475	0.017	3548	0.015	5817	0.013	7622	0.011	9755	0.010
with shim	FE multi layer*	2447	0.018	3508	0.017	5810	0.016	7638	0.013	9726	0.012
	FE hom*	2416	0.019	3543	0.014	5838	0.011	7698	0.011	9780	0.011
brake pad	Experimental	4045	0.024	5334	0.029	7373	0.027	9900	0.024		
with shim	FE hom*	4362	0.023	5731	0.025	7409	0.024	10061	0.031		

[a] bending mode, [b] torsional mode, * solid elements, ** shell elements

progression of the damping behavior correctly. Note that the first natural frequency in both cases is below the experimental determined frequency.

Regarding a complete brake pad the friction material behaves like a typical transversely isotropic material. Out-of-plane is the preferred direction of the lining characterized by less stiffness. The stiffness of the lining increases with piston pressure applied in normal direction. For Finite Element models engineering constants are used in Abaqus for describing the behavior for a certain pressure stage. Therefore experimental identified natural frequencies are lower than numerical computed ones listed here. Detailed information on this topic can be found e. g. in Hornig (2015). Beside this, the application of the homogenized shim structure enables to reduce the number of degrees of freedom. Figure 30.12 depicts the modeling advantage, whereby all components compared are meshed with the same element length. Two test objects, a rectangular plate with dimensions of 180x50x5 mm^3 fully covered with a shim and a backplate with the same shim type are listed. In particular quadratical solid elements (C3D20) and shell elements (S8R) are used for the considered structures. The number of elements needed for convergence is much less for homogenized models, which reduces the computation time drastically. The reduction of degrees of freedom is intended for large FE brake models often built with several million degrees of freedom. Achieving similar results using the homogenization theory, shims are highly recommended to be modeled as one layer over the thickness. Furthermore elements with full integration and second order approach are recommended preventing hourglass effects and shear locking as described in Flanagan and Belytschko (1981) and Bathe (1996). The analytical constrained layer damping approach provides a very good forecast quality for bending shapes. Solely the loss factor of the first bending mode deviates from the actual damping. Simple continuum mechanical approaches reflect only the stiffness characteristics of structures

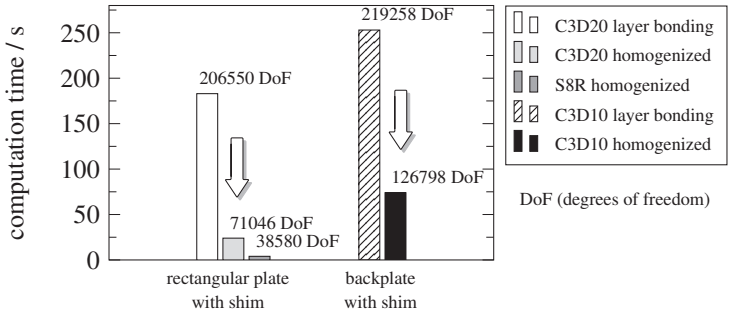

Fig. 30.12 Reduction of computation time due to improved single layer modeling

presented in Sect. 30.2.1. The results for torsional vibrations point out, that there has been simplified modeling for this application at increasing frequencies.

To sum up it can be said, that the results of the applied analytical and modified FE single layer approach conduct in very good compliance with the experimental investigations.

30.6 Conclusion and Outlook

The analytical constrained layer damping approach allows the prediction of natural frequencies and loss factors of bending mode shapes without considering relevant damping ratios carried out in prior investigations. Experimental evaluations of formal identical brake pads have shown, that there's a not neglectable deviation in the damping ability. Therefore the exact mapping of damping characteristics in Finite Element models is not feasible and favours the Rayleigh approach clearly. By modeling each layer separately the meshing becomes a challenging task due to the layer thickness. Therefore, the homogenization approach is the preferred modeling technique. A significant reduction of computation time for homogenized shim structures arose from a much lower number of degrees of freedom.

Primarily the advantage for future works is to reduce experimental investigations in a greater scope, improve the prediction quality of potential squeal frequencies and make the development of quiet brakes more efficient. The implementation of these homogenized shim structures in a FE complete model of the brake will be conducted in further steps. Furthemore the impact of varying temperature on shim loss factors has been depicted in prior examinations and can now be implemented in Finite Element calculations (Schmid et al, 2017).

Acknowledgements "This work is funded by the Deutsche Forschungsgemeinschaft (DFG, German Research Foundation) – WA 1427/27-1 within the PP 1897 "*Calm Smooth and Smart - Novel Approaches for Influencing Vibrations by Means of Deliberately Introduced Dissipation*". We would also like to thank Audi AG and Wolverine Advanced Materials for their support.

References

Bathe K (1996) Finite element procedures. Prentice-Hall Inc.
Beards C (1983) Structural vibration analysis. John Wiley and Sons New York
Beranek L, Vér I (1992) Noise and vibration control engineering: principles and applications. John Wiley & Sons, Inc.
Cantoni C, Cesarini R, Mastinu G, Rocca G, Sicigliano R (2009) Brake comfort - a review. Vehicle System Dynamics 47(8):901–947
Crandall S (1970) The role of damping in vibration theory. Journal of Sound and Vibration 11(1):3–18
DiTaranto R (1965) Theory of vibratory bending for elastic and viscoelastic layered finite-length beams. Journal of Applied Mechanics 32(4):881–886
Esgandari M, Olatunbosun O (2016) Computer aided engineering prediction of brake noise: modeling of brake shims. Journal of Vibration and Control 22(10):2347–2355
Ewins D (1984) Modal testing: theory and practice. Research studies press Letchworth
Festjens H, Chevallier G, Renaud F, Dion J, Lemaire R (2012) Effectiveness of multilayer viscoelastic insulators to prevent occurrences of brake squeal: A numerical study. Journal of Applied Acoustics 73(11):1121–1128
Flanagan D, Belytschko T (1981) A uniform strain hexahedron and quadrilateral with orthogonal hourglass control. International Journal for Numerical Methods in Engineering 17(5):679–706
Flint J (2002) Disc brake squeal. PhD thesis, University of Southern Denmark
Flint J, McDaniel J, Li X, Elvenkemper A, Wang A, Chen SE (2004) Measurement and simulation of the complex shear modulus of insulators. Tech. rep., SAE Technical Paper 2004-01-2799
Gräbner N, Tiedemann M, von Wagner U, Hoffmann N (2014) Nonlinearities in friction brake NVH - experimental and numerical studies (no. 2014-01-2511). SAE Technical Paper
Gräbner N, Gödecker H, von Wagner U (2015) On the influence of damping on brake vibrations. In: International Conference on Engineering Vibration
Gräbner N, Mehrmann V, Quraishi S, Schröder C, von Wagner U (2016) Numerical methods for parametric model reduction in the simulation of disk brake squeal. ZAMM-Journal of Applied Mathematics and Mechanics 96(12):1388–1405
Hagedorn P, DasGupta A (2007) Vibrations and waves in continuous mechanical systems. John Wiley & Sons
Hornig S (2015) Development of measurement and identification methods for automotive brake lining material properties in nvh relevant loading parameter range. PhD thesis, Technische Universität Berlin
Jones D (2001) Handbook of viscoelastic vibration damping. John Wiley & Sons
Kang J (2012) Finite element modelling for the investigation of in-plane modes and damping shims in disc brake squeal. Journal of Sound and Vibration 331(9):2190–2202
Kerwin Jr E (1959) Damping of flexural waves by a constrained viscoelastic layer. The Journal of the Acoustical Society of America 31(7):952–962
Kinkaid N, O'Reilly O, Papadopoulos P (2003) Automotive disc brake squeal. Journal of Sound and Vibration 267(1):105–166
Lall A, Asnani N, Nakra B (1988) Damping analysis of partially covered sandwich beams. Journal of Sound and Vibration 123(2):247–259
Lanczos C (1950) An iteration method for the solution of the eigenvalue problem of linear differential and integral operators. United States Governm. Press Office Los Angeles, CA
Lazan B (1968) Damping of materials and members in structural mechanics. Pergamon press Oxford
Leaderman H (1949) Proposed nomenclature for elastic and inelastic behavior of high polymers. Journal of Colloid Science 4(3):193–210
Marcelin JL, Shakhesi S, Pourroy F (1995) Optimal constrained layer damping of beams: experimental and numerical studies. Shock and Vibration 2(6):445–450

Markuš v (1974) Damping mechanism of beams partially covered by constrained viscoelastic layer. Acta Technica ČSAV 2:179–194

Mead D, Markuš v (1969) The forced vibration of a three-layer, damped sandwich beam with arbitrary boundary conditions. Journal of Sound and Vibration 10(2):163–175

Mead D, Markuš v (1970) Loss factors and resonant frequencies of encastré damped sandwich beams. Journal of Sound and Vibration 12(1):99–112

Nashif A, Jones D, Henderson J (1985) Vibration damping. John Wiley & Sons

Nokes D, Nelson F (1968) Constrained layer damping with partial coverage. Shock and Vibration Bulletin 38:5–10

Oberst H (1956) Werkstoffe mit extrem hoher innerer Dämpfung. Acta Acustica united with Acustica 6(1):144–153

Oberst H, Frankenfeld K (1952) Über die Dämpfung der Biegeschwingungen dünner Bleche durch fest haftende Beläge. Acta Acustica united with Acustica 2(4):181–194

Oberst H, Becker G, Frankenfeld K (1954) Über die Dämpfung der Biegeschwingungen dünner Bleche durch fest haftende Beläge II. Acta Acustica united with Acustica 4(1):433–444

Ottl D (1981) Schwingungen mechanischer Systeme mit Strukturdämpfung. VDI-Verlag

Rao D (1978) Frequency and loss factors of sandwich beams under various boundary conditions. Journal of Mechanical Engineering Science 20(5):271–282

Ross D, Ungar E, Kerwin Jr E (1959) Damping of plate flexural vibrations by means of viscoelastic laminae. Structural damping pp 49–97

SAE-J3001 (2011) Brake insulator damping measurement procedure. URL https://doi.org/10.4271/J3001_201102

Schmid D (2018a) Brake pad. "figshare.com/articles/Brake_pad/7046663", license CC BY 4.0, doi:110.6084/m9.figshare.7046663.v1

Schmid D (2018b) Shim test rig. "http://figshare.com/articles/Shim_test_rig/7046909", DOI "10.6084/m9.figshare.7046909.v1", license CC BY 4.0, doi:10.6084/m9.figshare.7046909.v1

Schmid D, Gräbner N, von Wagner U (2017) Experimental investigations of brake pad shim properties. PAMM 17(1):41–44

Sun C, Lu Y (1995) Vibration damping of structural elements, vol 1. Prentice Hall Englewood Cliffs, NJ

Sylwan O (1978) Calculation of partially covering damping layers of sandwich structures with some practical results. In: Proceedings from Inter-Noise-78, Institute of Noise Control Engineering, San Francisco, pp 219–224

Zienkiewicz O (1977) The finite element method, 3rd edn. McGraw-Hill London